

## Self-Assembly of Two-Dimensional Islands via Strain-Mediated Coarsening

Feng Liu,\* Adam H. Li, and M.G. Lagally

University of Wisconsin, Madison, Wisconsin 53706

(Received 11 May 2001; published 31 August 2001)

We demonstrate two distinctive effects of strain-induced island-island interaction on island size and spatial distribution during coarsening of 2D islands. When coarsening proceeds via only mass transport between islands, the interaction broadens the island size distribution, leading to a power-law dependence of island size uniformity on island number density. When coarsening proceeds via island migration in addition to mass transport between islands, the interaction can effectively direct island motion through island edge diffusion, leading to self-organized formation of a regular array of islands with both uniform size and spacing.

DOI: 10.1103/PhysRevLett.87.126103

PACS numbers: 81.15.Kk, 68.35.Md, 68.37.Lp

Self-assembly and self-organization of strained two- and three-dimensional (2D and 3D) islands in heteroepitaxial growth have recently been shown to provide an attractive route to nanofabrication of quantum dots (QDs). A prerequisite condition for their potential use as QDs is that they have a narrow size distribution. Coarsening, a fundamental process in the formation of a condensed phase of islands from a supersaturated 2D vapor phase of adatoms, can help to achieve island size uniformity [1–17], aided either thermodynamically by a strain-induced equilibrium stable island size [6–12] or kinetically by self-limiting effects [13,14]. Previous theoretical studies have focused on the influence of strain on island size stability; very little attention has been paid to its influence on the island size and spatial distributions. Initial configurations of islands with a uniform size and spatial distribution have been assumed. For example, thermodynamic analyses, whether 2D [6,9] or 3D [10,11], have been carried out on a periodic array of equal-sized islands to investigate their stability against coarsening (Ostwald ripening) to form a sparser array of equal-sized larger islands or a single larger island.

In actual film growth, islands, of course, nucleate randomly at different positions and grow into different sizes. This initial randomness can have significant effects on the coarsening behavior in the presence of strain, especially when all physical manifestations of strain are included. In this Letter, we demonstrate how strain-induced island-island interactions influence coarsening of a random array of islands. These effects will manifest themselves *if and only if* the initial distribution of island size and spacing is random. We demonstrate that strain can influence not only the mass transport between islands but also the mass transport within 2D islands, thereby triggering a self-organization that narrows the island size distribution. We show that the strain-induced island-island interaction manifests itself in two different influences on coarsened island size and spatial distribution, depending on the form of mass transport involved in the coarsening process. If only strain-modified mass transport between 2D islands is added to the coarsening process, the strain-induced interaction *broadens* the island size distribution. The width

of the broadening increases with decreasing island number density, in a power-law dependence. If mass transport within an island (i.e., via island edge diffusion; hence, islands are effectively migrating during coarsening) is included in addition to mass transport between islands, the interaction can influence the direction of island edge diffusion and effectively lead to a strain-directed island motion. This motion, combined with a thermodynamic driving force to reach the strain-induced stable island size, can then drive a random array of 2D islands to self-organize, forming a triangular lattice of islands with greatly improved uniformity in island size and spacing.

In general, island coarsening may proceed with or without island migration. Without island migration, coarsening is governed solely by chemical potentials of individual islands, which then control the mass transport between islands. Consider an array of coherently strained 2D circular islands (Fig. 1), formed at the early stage of heteroepitaxial growth in the submonolayer regime. The total energy of a single island (neglecting the island-island interaction for now) can be calculated as the sum of the step energy and island strain energy:

$$E_i^{\text{sin}}(R_i) = (2\pi R_i) \left[ \sigma - \alpha \ln \frac{R_i}{a_0} \right], \quad (1)$$

where  $R_i$  is the radius of the  $i$ th island and  $\sigma$  is the island edge (step) energy.  $\alpha = 4\pi F^2(1 - \nu^2)/\mu$  is related to the misfit strain-induced elastic force monopole ( $F$ ) along the island edge and elastic constants  $\nu$  (Poisson ratio) and  $\mu$  (Young's modulus).  $a_0$  is a cutoff length, of the order of a surface lattice constant. The chemical potential of a single island is then

$$u_i^{\text{sin}}(R_i) = \nu \left[ \frac{\sigma - \alpha}{R_i} - \frac{\alpha}{R_i} \ln \frac{R_i}{a_0} \right], \quad (2)$$

where  $\nu$  is the surface area per atom in the island.

Without strain (as in homoepitaxy), the island chemical potential is inversely proportional to its size, and coarsening leads to a continuous increase of average island size indefinitely. Strain introduces an island size that is thermodynamically stable against further coarsening. From

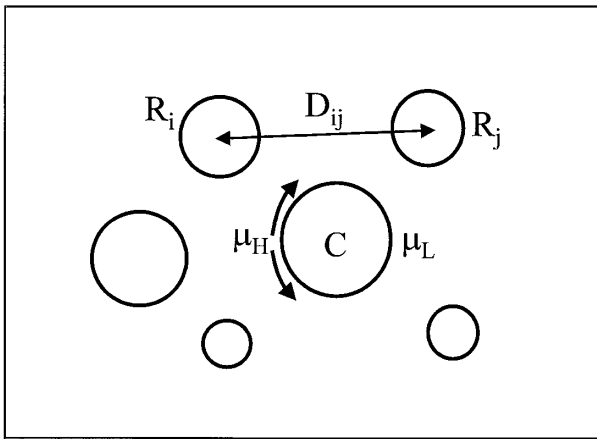


FIG. 1. Schematic diagram of an array of circular 2D islands.  $R_i$  and  $R_j$  denote the radius of the  $i$ th and the  $j$ th islands, respectively, with a separation  $D_{ij}$ . The island at the center labeled C has three neighbors on the left and two on the right. The chemical potential on its left-side edge ( $\mu_H$ ) is higher than on the right-side edge ( $\mu_L$ ), i.e.,  $\mu_H > \mu_L$ , because of the strain-induced island-island interaction. The two arrows on its left edge indicate the direction of net mass flow via edge diffusion, causing effectively an island drifting toward the right.

Eq. (2), the island chemical potential has a minimum of  $u_0 = (\nu\alpha)/R_0$ , at  $R_0 = a_0 e^{\sigma/\alpha}$ . Consequently, coarsening will tend to drive all the islands toward this stable size, forming a uniform island size distribution. (At finite temperatures, the contribution of entropy broadens the island sizes into a Gaussian distribution [8] and moves the mean island size away from  $R_0$  [18].)

Strain also induces an elastic interaction between islands, which will further modify the island chemical potential and, hence, changes the coarsening behavior of an island array. This additional interaction energy contribution to the  $i$ th island can be calculated as

$$\Delta E_i^{\text{int}}(R_i) = (2\pi\beta) \sum_{j \neq i} \frac{R_i^2 R_j^2}{D_{ij}^3}, \quad (3)$$

where  $R_j$  is the radius of the  $j$ th island,  $D_{ij}$  is the separation between the  $i$ th and the  $j$ th islands, and  $\beta = F^2(1 + \nu^2)/2\mu$ . To arrive at Eq. (3), we assume the size,  $R$ , of islands is much smaller than their separation,  $D$ , so that the higher-order interaction terms are neglected. Correspondingly, the correction to the chemical potential of the  $i$ th island is

$$\Delta u_i^{\text{int}}(R_i) = \nu\beta \sum_{j \neq i} \frac{R_j^2}{D_{ij}^3}. \quad (4)$$

The interaction makes the chemical potentials of the islands dependent on their environment (i.e., the size and position of neighboring islands). Because the islands, in general, nucleate at random positions during epitaxial growth, with different neighboring island configurations, they will converge in a coarsening process to different stable sizes,  $R_i$ , rather than to the same size,  $R_0$ , for

strained islands without island-island interaction. Consequently, the equilibrium island size distribution is broader than that obtained without considering the interaction.

As coarsening drives the system toward equilibrium, all the islands reach the same chemical potential, so

$$u_i^{\text{sin}}(R_i) + \Delta u_i^{\text{int}}(R_i) = \text{const.} \quad (5)$$

For  $R \ll D$ , the limit we are considering, we have  $\Delta u_i^{\text{int}} \ll u_i^{\text{sin}}$ ; i.e., the interaction is a small correction to the total island chemical potential. The stable island size including the interaction,  $R_i$ , is close to the minimum without the interaction,  $R_0$ . We can approximate  $u_i^{\text{sin}}$  using its Taylor expansion up to the second order,

$$\begin{aligned} u_i^{\text{sin}}(R_i) &= u_i^{\text{sin}}(R_0) + \frac{1}{2} \left( \frac{d^2 u_i^{\text{sin}}}{dR_i^2} \right) \Big|_{R_i=R_0} (R_i - R_0)^2 \\ &= u_0 + c_2(\Delta R)^2. \end{aligned} \quad (6)$$

Furthermore, because  $\Delta u_i^{\text{int}}$  decays as  $D^{-3}$ , we take only the nearest-neighbor interaction,

$$\Delta u_i^{\text{int}}(R_i) = \nu\beta \sum_{j \neq i} \frac{R_{\text{NN}}^2}{D_{\text{NN}}^3} = k \frac{\bar{R}^2}{\bar{D}^3} = k \bar{R}^2 n^{3/2}. \quad (7)$$

To derive Eq. (7), we assume the islands are distributed on the surface with a spatially uniform average number density of  $n$ . From dimensional arguments, we have  $\bar{D} \propto \sqrt{1/n}$  [19]. Substituting Eqs. (6) and (7) into (5), we have

$$\frac{\Delta R}{\bar{R}} \sim n^{3/4}. \quad (8)$$

Therefore, the width of the island size distribution (i.e., the size deviation,  $\Delta R$ , from  $R_0$ ) caused by the strain-induced island-island interaction scales with island number density in a power law with an exponent of  $\frac{3}{4}$ . As the island density increases, the islands get closer, and the island-island interactions get stronger. Consequently, the islands are driven farther away from the stable size without island-island interaction,  $R_0$ , and the width of their size distribution,  $\Delta R$ , increases.

Computer simulations of coarsening of strained 2D islands confirm quantitatively the power-law dependence of the width of the island size distribution on number density. In a standard coarsening process, in which mass transport between islands is limited by attachment/detachment of adatoms to/from island perimeters, the rate of change of island size can be expressed as

$$\frac{dR_i}{dt} = C_{\text{AD}}(\bar{u} - u_i), \quad (9)$$

where  $C_{\text{AD}}$  is a coefficient related to the adatom attachment/detachment rate and the atomic area.  $\bar{u}$  is the mean chemical potential averaged over all the islands. We start the simulations with a random distribution of island sizes and positions, to mimic the initial island nucleation and subsequent growth. At each time step, the chemical

potential of each island is calculated, including the contribution from island-island interactions, and the island sizes are updated according to Eq. (9). Periodic boundary conditions are employed in calculating the island-island interaction, using a cutoff distance slightly larger than half of the simulation cell size. (Because the interaction scales inversely with the third power of island separation, the convergence is guaranteed in two dimensions.) Figures 2(a) and 2(b) show the typical initial and final island configurations. Figure 3(a) shows the time evolution of the island size distribution. At time  $t = 0$ , the island sizes are randomly chosen between 0 and 100. As time proceeds, small islands evaporate quickly, while medium and large islands converge into a narrow size distribution around the optimum size,  $R_0 = 76$ . For a given island number density, the width of the converged island size distribution is determined by averaging over a great number of runs starting with different initial island configurations of the same number density. Figure 3(b) shows the simulated width of the island size distribution as a function of island number density. In the low-density limit, the width scales with density in a power law with an exponent of  $\frac{3}{4}$ , in excellent agreement with the analytical solution. The power law fails at higher densities, because the assumption that island separation is much smaller than island size no longer holds and higher-order interaction terms become significant.

Next, we consider coarsening with island migration. The strain-induced island-island interaction not only changes the average chemical potential of an island, but also introduces a chemical potential gradient within the island. In a random island array, the configuration of neighboring islands of a given island is, in general, anisotropic. For example, in Fig. 1, there are three neighboring islands on the left side of the center island (labeled island C) but only two islands on the right. Consequently, the center island feels a stronger interaction from the left and the chemical potential is higher along its left edge

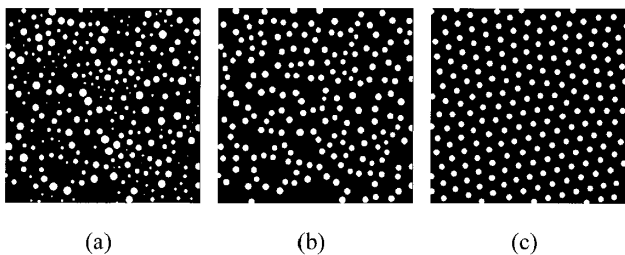


FIG. 2. Snapshots of simulated island configurations. (a) The initial configuration with random island sizes and positions. (b) The final converged island configuration from coarsening simulations *without* island migration, using the initial configuration of (a). (c) The final converged island configuration from coarsening simulations *with* island migration, using the initial configuration of (a). The islands form a triangular lattice with much improved size and spatial uniformity relative to those in (b).

( $u_H$ ) than along the right edge ( $u_L$ ). As the island-island interaction is repulsive, it gives rise to a positive contribution to the chemical potential. This chemical-potential gradient will then direct a net mass flow from the left edge to the right edge on the center island, if edge diffusion is activated (comparable to surface diffusion) during coarsening, effectively driving the island to move toward the right.

We have incorporated such strain-directed island motion into simulations to investigate its influence on coarsening. At each time step, in addition to mass exchange between islands that is determined by the average island chemical potential, we calculate the gradient of chemical potential at the center of each island and let the island drift along the gradient direction. The speed of island motion is set to be proportional to the magnitude of the gradient and inversely proportional to the island radius. (A larger island moves more slowly than a smaller island, because it takes longer for the atoms to travel the distance of the island perimeter for an island to move one atomic unit.) Figure 2(c) shows the final island configuration simulated from the initial configuration of Fig. 2(a). The islands form a

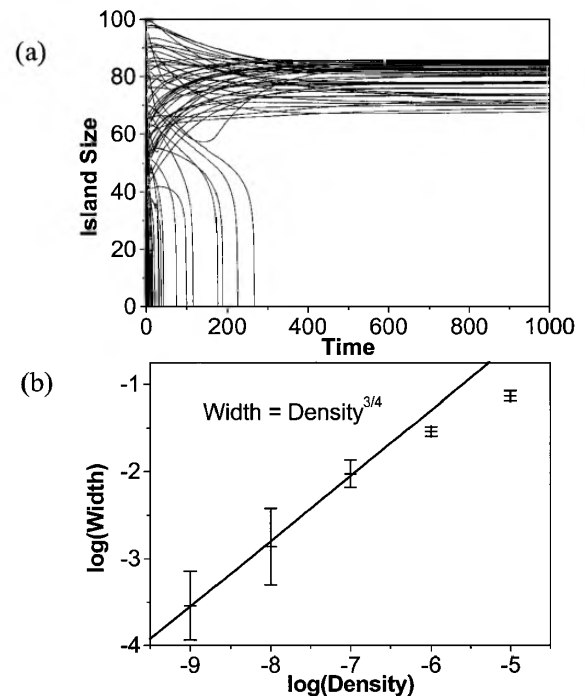


FIG. 3. (a) Time evolution of the island size distribution from a typical simulation of coarsening without island migration. The initial size distribution is represented by the  $y$  intercepts at  $t = 0$ . Islands may grow (shrink) first and then shrink (grow). In general, the smallest islands disappear (dissolution), while larger islands may either grow or shrink. All converge toward a finite size distribution centered around  $R_0 = 76$ . (b) Log-log plot of the width of the island size distribution as a function of island number density. The straight line is a linear fit to the simulation data using the slope of  $\frac{3}{4}$ . The error bars on the data reflect averaging over many different runs.

triangular lattice, neglecting the effect of substrate symmetry as isotropic step energy and diffusion are assumed in the simulation, with much improved spatial and size uniformity, compared to the final configuration in Fig. 2(b), which was simulated from the same initial configuration [Fig. 2(a)] but without island motion.

The obvious degeneracy of several domains of triangular lattice with different orientations indicates that the ordering originates locally in different regions, forming patches of different orientations; domain boundaries (or dislocations) are formed when these patches meet. The much improved island size uniformity correlates with the spatial uniformity. As the repulsive island-island interaction drives the island into a close-packed ordered array, the local environment of an island becomes more uniform; every island has a similar hexagonal neighboring island configuration and, hence, converges toward an almost equal stable island size.

This self-organization, induced by strain-directed island motion during coarsening, provides the most plausible mechanism and pathway for the formation of a triangular lattice of Ag vacancy islands on Ru(0001) observed in a recent experiment by Pohl *et al.* [1]. They show that an isolated vacancy island is very mobile and the interaction between vacancy islands is elastic in nature, conclusions that are completely consistent with the physical assumptions of our model. The simulations show that the self-organized ordering is more effective at higher island number densities when the island-island interaction is stronger, in good agreement with experimental observations [1] that islands form only a triangular lattice at sufficiently high island density. The fast-rising island-island repulsion at a short distance effectively suppresses the coalescence of islands during coarsening, as observed in both experiment [1] and simulation. The island size distribution is broader in the experimental lattice than in the simulated lattice, primarily because thermal broadening is not included in the simulation.

In summary, we have demonstrated, by both theoretical analysis and computer simulation, that strain-induced island-island interactions can have distinctive effects on two standard coarsening processes in arrays of 2D islands. For coarsening without island motion, the interaction gives rise to a universal power-law dependence of the island size distribution on island number density with an exponent of  $\frac{3}{4}$  when the island density is low. Thus far, to the best of our knowledge, there are no experiments to compare to this prediction. For coarsening with island motion, via island edge diffusion, the interaction directs the island motion, leading to the self-organized formation

of a regular lattice of islands with uniform island size. The self-organization explains not only the formation of a triangular lattice of Ag vacancy islands on Ru(0001) [1] but is also likely to be a general mechanism in other strain-driven growth systems. It provides a unique method for creating nanoscale templates with uniform size and spacing for patterning and growth of nanostructures.

This work was supported by DOE, Grant No. DE-FG03-01ER45875, and by NSF, Grant No. DMR-9632527.

---

\*Present address: University of Utah, Salt Lake City, UT 84112.

Electronic address: fliu@eng.utah.edu

- [1] K. Pohl, M.C. Bartelt, J. de la Flguera, N.C. Bartelt, J. Hrbek, and R.Q. Hwang, *Nature (London)* **397**, 238 (1999).
- [2] F.M. Ross, J. Tersoff, and R.M. Tromp, *Phys. Rev. Lett.* **80**, 984 (1998).
- [3] S. Lee, I. Daruka, C.S. Kim, A.-L. Barabási, J.L. Merz, and J.K. Furdyna, *Phys. Rev. Lett.* **81**, 3479 (1998).
- [4] G.R. Carlow and M. Zinke-Allmang, *Phys. Rev. Lett.* **78**, 4601 (1997).
- [5] J. Drucker, *Phys. Rev. B* **48**, 18 203 (1993).
- [6] V.I. Marchenko, *JETP Lett.* **33**, 381 (1981).
- [7] J. Tersoff and R.M. Tromp, *Phys. Rev. Lett.* **70**, 2782 (1993).
- [8] C. Priester and M. Lannoo, *Phys. Rev. Lett.* **75**, 93 (1995).
- [9] K. Ng and D. Vanderbilt, *Phys. Rev. B* **52**, 2177 (1995).
- [10] V.A. Shchukin, N.N. Ledentsov, P.S. Kop'ev, and D. Bimberg, *Phys. Rev. Lett.* **75**, 2968 (1995).
- [11] I. Daruka and A.-L. Barabási, *Phys. Rev. Lett.* **79**, 3708 (1997).
- [12] G. Medeiros-Ribeiro, A.M. Bratkovski, T.I. Kamins, D.A. Ohlberg, and R.S. Williams, *Science* **279**, 353 (1998).
- [13] Y. Chen and J. Washburn, *Phys. Rev. Lett.* **77**, 4046 (1996); A.-L. Barabási, *Appl. Phys. Lett.* **70**, 2565 (1997).
- [14] D.E. Jesson, G. Chen, K.M. Chen, and S.J. Pennycook, *Phys. Rev. Lett.* **80**, 5156 (1998); M. Kästner and B. Voigtländer, *Phys. Rev. Lett.* **82**, 2745 (1999).
- [15] J.A. Floro, E. Chason, M.B. Sinclair, L.B. Freud, and G.A. Lucadamo, *Appl. Phys. Lett.* **73**, 951 (1997).
- [16] J.A. Floro, M.B. Sinclair, E. Chason, L.B. Freud, R.D. Twisten, R.Q. Hwang, and G.A. Lucadamo, *Phys. Rev. Lett.* **84**, 701 (2000).
- [17] For a review on 3D island stability, see V.A. Shchukin and D. Bimberg, *Rev. Mod. Phys.* **71**, 1125 (1999).
- [18] V.A. Shchukin *et al.*, *Phys. Status Solidi (b)* **224**, 503 (2001).
- [19] More rigorously, we can calculate the probability of finding a nearest neighbor at distance  $D$  for a random distribution to be  $P(D) = 2\pi nD \exp(-\pi nD^2)$  and  $\overline{D} \propto \sqrt{1/n}$ .